AIMS Mathematics, 10(4): 10204–10227.
DOI: 10.3934/math.2025465
Received: 25 February 2025
Revised: 15 April 2025
Accepted: 22 April 2025
Published: 29 April 2025

http://www.aimspress.com/journal/Math

Research article

Modeling and numerical simulation of Lumpy skin disease: Optimal control dynamics approach

Awatif J. Alqarni*

Department of Mathematics, College of Science, University of Bisha, P.O. Box 551, Bisha, 61922, Saudi Arabia

* **Correspondence:** Email: aaljhman@ub.edu.sa.

Abstract: In this research, I aimed to develop a mathematical system that simulates the mechanics of lumpy skin disease (LSD) transmission in cattle. The approach of optimal control was used, and the samples were divided into six categories: Infected, recovered, susceptible, vaccinated, susceptible vector insects, and infected vector insects. The Runge-Kutta technique from the fourth order was used to solve the numerical system, and the effects of various preventative actions like treatment, vaccination, and pesticide spraying on the dissemination of the disease were studied. The stability of the mathematical model was investigated, and it was determined that the disease-free equilibrium point is stable when the infection fails to spread within the population. A sensitivity analysis was performed, and the results showed that the exceedingly sensitive parameters are the natural mortality rate of vector insects and the vaccination rate. The hypothesis of optimal control was used to identify the optimal strategies to reduce the disease's proliferation, and it was found that the combination of all measures significantly reduces the number of infected cases and is a reason for increasing the number of recovered cattle, emphasizing the significance of other measures like early vaccination and isolation of infected cattle.

Keywords: Lumpy skin disease model; optimal control problem; stability analysis; sensitivity analysis; numerical simulation
Mathematics Subject Classification: 93C10, 92B05, 90C31, 34D20

1. Introduction

LSD is a highly contagious viral disease of cattle. The Neethling virus, a member of the Capripoxvirus genus, is the cause of it. The sickness is accountable for the significant reduction in dairy components. Once LSD proliferates among a population, the agricultural society may encounter significant losses due to animals experiencing abortions, weight reduction, and diminished fertility. It could potentially result in irreversible harm to the skin. LSD is listed as a notifiable disease by the World Organization for Animal Health. Notifiable illnesses are those that must be reported within a specified timeframe upon identification by veterinarians or owners [1]. Although cattle are the primary animal susceptible to LSD, experimental infections indicate that the virus can also infect sheep, goats, giraffes, gazelles, and impalas. The designation LSD derives from the observation that the lymph nodes of the diseased animal enlarge and appear as lumps on the skin. Significant cutaneous nodules develop on the neck, udder, head, abdomen, limbs, and genitalia of infected cattle, subsequently progressing to ulcers and ultimately transforming into skin scabs [2]. The sickness evolves within 4 to 14 days [3]. The utilization of attenuated viruses for immunization has proven to be an effective strategy in controlling LSD [4]. Inoculation with tainted or inadequately attenuated vaccinations can precipitate outbreaks of lumpy skin disease [5]. The restricted availability of vaccinations complicates the control of LSD in many regions [6]. Alternative strategies such as killing affected animals, imposing movement restrictions, and implementing vector control have been employed; however, their efficacy in the absence of immunization has been inconsistent [7]. Therefore, it is crucial to identify additional intervention measures to complement immunization efforts in order to reduce LSD transmission patterns. The documented use of LSD in several countries throughout diverse global regions. The ailment was originally widespread in Africa, especially in sub-Saharan nations. The initial recorded instances of LSD occurred in Zambia and Kenya during the 1920s and the 1930s, in turn. LSD later spread to several African countries, such as Uganda, Tanzania, Sudan, Ethiopia, and South Africa. Over the past few years, its geographic range has extended beyond Africa. Outbreaks have been documented in nations throughout Europe, Asia, and the Middle East. Many European countries, including Albania, North Macedonia, Serbia, Bulgaria, and Greece, have confirmed incidences of LSD. The nations of the Middle East, Saudi Arabia, Iraq, and Jordan, have also detected the disease [1].

Models for mathematically describing epidemic diseases serve a crucial role in epidemiology. A range of epidemic systems is being created and utilized for the investigation and management of numerous diseases, including AIDS/HIV [8], cholera [9], Ebola virus [8,10], TB [11], and COVID-19 [12,13]. Another objective of epidemic disease modeling is to understand the long-term dynamics of the disease and to identify requisite management methods [14]. Comprehending the transmission patterns of an infectious disease is essential for formulating effective control strategies. Numerous modeling studies employing epidemic data have sought to improve the comprehension of LSD transmission dynamics by including the rates of incubation, recruitment, vaccination, [15–17] and essential dynamics (birth and natural mortality) [18,19]. The incidence of LSD has been predicted using time series analysis and demographic projections in [20,21]. In [22], the authors developed an LSD nonlinear fractional system that excludes the exposed category, but in [14], the vector population is disregarded. In [23], the authors examined both populations of cattle and vectors but did not factor in the decline of infection-induced immunity. Certain studies in 2019 on the malaria and the coronavirus disease (COVID-19) have included the decline in immunity rate after recovery, highlighting the significance of this factor in the transportation dynamics of epidemic diseases

characterized by recurrent incidence (re-infection following recuperation) [24]. Optimal control theory is utilized not just in engineering and several scientific disciplines but is also regarded as particularly beneficial in modeling disease epidemic control. This theory encompasses significant principles that delineate how disease in a particular or extensive zone can be managed using proposed or existing biological controls. Numerous scholars applied this approach to epidemic models for potential infection control. To eradicate illness from society, researchers developed various mathematical models incorporating control variables and effective tactics. In recent decades, various control models have been presented to eliminate infections from different diseases, including the model of Okosun and Makinde, which examines the co-infection of cholera and malaria to analyze their interacting behavior [25]. Ullah and Khan have developed a model of optimal control for the new COVID-19 epidemic and examined the data presented in Pakistan [26]. They determined that the sickness could be mitigated by implementing of the suggested control techniques.

Research has shown the effectiveness of fractional-order models in capturing memory effects in epidemic transmission. These models offer promising insights into diseases with long-term dependencies, such as those found in [27,28], suggesting a potential direction for future extensions of this classical LSD model. By applying the theory of optimal control to their controlled transmission dynamics system, Khan et al. investigated the effects of isolation, treatment, and vaccine on infection reduction. They concluded that the controls were helpful [29]. The fractional order model based on the Atangana-Baleanu derivative was constructed to describe the LSD dynamics in [30], and formulate an optimal control problem involving vaccination and quarantine control strategies.

In [30] demonstrated the effectiveness of both pharmaceutical and non-pharmaceutical controls in mitigating the spread of LSD. This was achieved by replacing a constant treatment rate with a time-dependent function and introducing a new time-varying parameter to model precautionary measures. However, the proposed mathematical model in [30] does not account for nonlinear interactions with insect vector species, leaving important gaps in understanding transmission dynamics. This raises several critical questions: How does including of biting flies as potential virus carriers influence the model's behavior? Could alternative control strategies be designed to target vector populations more effectively? I aim to address these unresolved questions and explore their implications for disease control.

I aim to extend the LSD model presented in [31] by proposing crucial improvements over previous studies [30] and [31] as follows:

(1) Incorporating the state variables of biting insects (vector compartments) into the proposed LSD mathematical model, thereby directly accounting for their epidemiological interactions with cattle populations.

(2) Formulating a mathematical framework contains three control measures, which are defined as vaccination control measures, treatment measures and quarantine of infected cattle, and pesticide spray measures for vectors to control the transmission dynamics of LSD disease.

(3) Constructing and solving a full optimal control problem using Pontryagin's Maximum Principle.

(4) Deriving the adjoint system and characterizing the optimal controls analytically.

(5) Investigate four optimal control strategies, each with detailed simulation and interpretation.

This article presents a mathematical framework for the LSD model that categorizes the population into six compartments: Susceptible cattle, vaccinated cattle, infected cattle, recovered cattle, susceptible vector, and infected vector. The objective is to create a dependable model to assess the impact of control measures on disease management by evaluating various control strategies. The model's validity

assessed by demonstrating a unique, positive, and bounded solution. Furthermore, the local stability of the suggested model at equilibrium points is shown. Analysis of sensitivity is used to identify the parameters of the model most sensitive to the reproduction number, which may enhance disease control efforts. Another impetus is to investigate various LSD management options by constructing an optimal control problem that contains vaccination, quarantine, and pesticide spray control measures to present different control strategies that reduce the transmission of LSD. To my knowledge, the work described in this paper has never been done before to limit the spread of LSD.

The organization of the paper is as follows: In Section 2, I delineate the formulation of a nonlinear and coupled mathematical model for LSD. In Section 3, I display the model's reliability by demonstrating the existence of a unique solution, along with the positivity and boundedness of the state variables. In Section 4, I include computations for the equilibrium locations and the calculations for the fundamental reproduction number R_0. Additionally, I conduct a stability study of the equilibrium points concerning R_0. In Section 5, a sensitivity analysis of the parameters of the model associated with the reproduction number R_0 is conducted. In Section 6, I design an ideal control strategy for effective illness management. Section 7 contains the results and discussions, while the conclusions of this article are encapsulated in Section 8.

2. Formulation and description of the mathematical model

Mathematical models can provide significant analysis for disease transmission dynamics. Moreover, a realistic model may aid in forecasting the disease's pattern and assist researchers in determining the best strategy for halting its spread. Therefore, in this section, a mathematical formulation of a model describing the transition dynamics of LSD is provided. The mechanics of the disease's transmission is the first goal, followed by a discussion of the control measures that can be taken to slow the disease's progress. How the LSD is transmitted is shown in Figure 1.

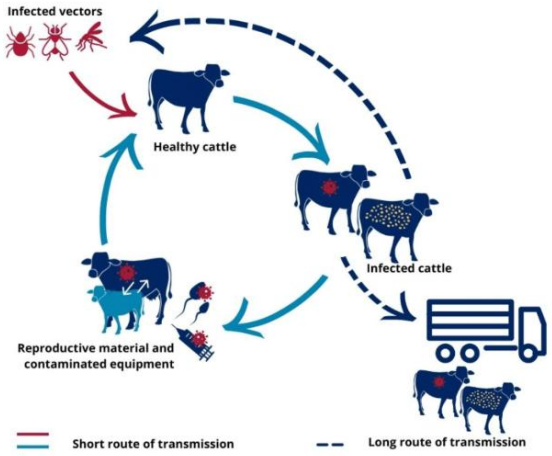

Figure 1. LSD model transmissions [32].

In this formulation, the total population of cattle N_C is subdivided into susceptible cattle S_C, which represents the cattle at risk of contracting the virus and getting sick by interacting with infected cattle, vaccinated V_C represents the cattle that are vaccinated. Infected cattle I_C, which stands as the category

of cattle in which the virus, settles and becomes infectious and transmits the disease. Recovered cattle R_C represents the cattle category that recovers quickly due to its high immunity or good treatment. The infection between cattle occurs due to vector insects such as mosquitoes, flies, or ticks. The total vector populations are indicated by N_V which are partitioned into susceptible S_V insects and infected insects I_V. During the hot and muggy summer and fall months, when flies are most common, the disease can spread quickly. Also, three control measures are incorporated to control the spread of infection transmission, where u_1 indicates vaccination control measures, u_2 indicates treatment measures and, quarantine of infected cattle, and u_3 indicates pesticide spray measures for vectors.

Based on the previously mentioned considerations, the dynamics of the LSD model can be represented by the next mathematical system:

$$\begin{aligned}
\frac{dS_C(t)}{dt} &= \Pi_1 - \frac{(1-u_2)\eta_1 S_C I_C}{N_C} - \frac{(1-u_3)\eta_2 S_C I_V}{N_C} - (\varepsilon + \gamma_1 + u_1)S_C + \alpha R_C,\\
\frac{dV_C(t)}{dt} &= (\varepsilon + u_1)S_C - \gamma_1 V_C,\\
\frac{dI_C(t)}{dt} &= \frac{(1-u_2)\eta_1 S_C I_C}{N_C} + \frac{(1-u_3)\eta_2 S_C I_V}{N_C} - (\rho + \gamma_1 + \sigma + u_2)\, I_C,\\
\frac{dR_C(t)}{dt} &= (\rho + u_2)I_C - (\alpha + \gamma_1)R_C,\\
\frac{dS_V(t)}{dt} &= \Pi_2 - \frac{(1-u_3)\eta_3 S_V I_C}{N_C} - (\gamma_2 + u_3)S_V,\\
\frac{dI_V(t)}{dt} &= \frac{(1-u_3)\eta_3 S_V I_C}{N_C} - (\gamma_2 + u_3)I_V.
\end{aligned} \tag{1}$$

Furthermore, the initial conditions are

$$S_C(0) > 0,\ V_C(0) \geq 0,\ I_C(0) \geq 0,\ R_C(0) \geq 0, \qquad S_V(0) > 0,\ {}_V(0) \geq 0,$$

where the model parameters are illustrated in Table 1.

Table 1. Values and explanation of the parameters for the LSD model [31].

Parameter	Description	value
Π_1	Birth rate of cattle	0.5
η_1	Contact rate between I_C and S_C	0.2
η_2	Contact rate between I_V and S_C	0.3
ε	Cattle vaccination rate	0.001
α	Waning rate of vaccination	0.01
γ_1	Cattle's natural death rate	0.0002
ρ	The recovery rate of cattle	0.07
Π_2	Recruitment rate of vector	50
γ_2	Vector's natural death rate	0.02
η_3	Contact rate between S_V and I_C	0.22
σ	Cattle mortality rate caused by disease	0.027

3. Mathematical analysis of the LSD model

In this section, I present theorems demonstrating that the LSD model (1) possesses a unique solution. I include fundamental concepts and theorems from functional analysis to support the demonstration of the theorems presented [14,23,24].

3.1. Existence of a unique solution

Let the LSD model (1) reform into the specified format.

$$\frac{dX}{dt} = F\big(X(t)\big),\ X(0) = X_0, \tag{2}$$

where $X(t) \in C^1[0,T]$ and $X(t)$: $\mathbb{R}_+ \to \mathbb{R}_+^6$ is a real-valued function that is defined by

$$X(t) = \big(S_C(t), V_C(t), I_C(t), R_C(t), S_V(t), I_V(t)\big)^T,$$

with

$$X_0 = \big(S_C(0), V_C(0), I_C(0), R_C(0), S_V(0), I_V(0)\big)^T,$$

and

$$F\big(X(t)\big) = \Big(F_1\big(X(t)\big), F_2\big(X(t)\big), F_3\big(X(t)\big), F_4\big(X(t)\big), F_5\big(X(t)\big), F_6\big(X(t)\big)\Big)^T.$$

Theorem 1. Assume that the function $F(X)$ satisfies the Lipschitz condition $\|F(X_2) - F(X_1)\|_\infty \leq h\,\|X_2 - X_1\|_\infty$, Consequently, Eq (2) possesses a unique solution for $H = hT < 1$.

Proof. The proof of this theorem follows the same manner as Theorem 6 in [14].

3.2 Boundedness and positivity of solutions

In this section, I demonstrate the boundedness and positivity of the model's state variables (1) and delineate the feasible region for these variables.

Theorem 2. Consider the starting information, denoted as $X(0) \geq 0$, where $X(t) = \big(S_C(t), V_C(t), I_C(t), R_C(t), S_V(t), I_V(t)\big)^T$. The solutions of system (1) with positive initial conditions stay positive for all $t \geq 0$. With $N_C(t) = S_C(t) + V_C(t) + I_C(t) + R_C(t)$ and $N_V(t) = S_V(t) + I_V(t)$.

Proof. It is assumed that $X(0) \geq 0$. Examine the first equation:

$$\frac{dS_C}{dt} = \Pi_1 - \left(\frac{(1-u_2)\eta_1 I_C}{N_C} + \frac{(1-u_3)\eta_2 I_V}{N_C} + \varepsilon + \gamma_1 + u_1\right) S_C + \alpha R_C.$$

It has been demonstrated that all state variables are constrained. Therefore, let

$$\xi = sup\left[\frac{(1-u_2)\eta_1 I_C}{N_C} + \frac{(1-u_3)\eta_2 I_V}{N_C} + \varepsilon + \gamma_1 + u_1\right].$$

Then $\frac{dS_C}{dt} \geq \Pi_1 - \xi S_C(t)$.

Application of the Laplace transform on both sides yields the following result:

$$sS_C(s) - S_{C_0} \geq \frac{\Pi_1}{s} - \xi S_C(s) \Longrightarrow S_C(s) \geq \frac{\Pi_1}{s(s+\xi)} + \frac{S_{C_0}}{(s+\xi)}.$$

Through the utilization of the inverse Laplace transform gives:

$$S_C(t) \geq \frac{\Pi_1}{\xi}\left(1 - e^{-\xi t}\right) + S_{C_0}e^{-\xi t}.$$

Since $0 < e^{-\xi t} \leq 1$ and $S_{C_0}e^{-\xi t} \geq 0$, hence it is evident that $S_C(t) \geq 0\ \forall t \geq 0$.

Likewise, this can be demonstrated for another state variable. Therefore, the viable region for the proposed model (1) is defined by

$$\Omega = \Psi_C \times \Psi_V, \text{ where } \Psi_C = \left\{\left(S_C(t), V_C(t), I_C(t), R_C(t)\right) \in \mathbb{R}_+^4 : 0 \leq N_C \leq \frac{\boldsymbol{\Pi_1}}{\gamma_1}\right\}$$

and

$$\Psi_V = \left\{\left(S_V(t), I_V(t)\right) \in \mathbb{R}_+^2 : 0 \leq N_V \leq \frac{\Pi_2}{(\gamma_2 + u_3)}\right\}.$$

Theorem 3. The solution $X(t) = \left(S_C(t), V_C(t), I_C(t), R_C(t), S_V(t), I_V(t)\right)^T$ of the LSD model (1) is bounded.

Proof. The aggregate populations of cattle and mosquitoes are

$$N_C(t) = S_C(t) + V_C(t) + I_C(t) + R_C(t), \tag{3}$$

$$N_V(t) = S_V(t) + I_V(t). \tag{4}$$

First, Eqs (3) and (4) are differentiated based on time t. This lets us get the next equation from the system of ordinary differential equations (1) on the right-hand side

$$\frac{dN_C}{dt} = \Pi_1 - \sigma I_C - \gamma_1 N_C, \tag{5}$$

$$\frac{dN_V}{dt} = \Pi_2 - (\gamma_2 + u_3)N_V, \tag{6}$$

with $N_C(0) = S_C(0) + V_C(0) + I_C(0) + R_C(0)$ and $N_V(0) = S_V(0) + I_V(0)$.

Eqs (5) and (6) can be expressed in the subsequent forms:

$$\frac{dN_C}{dt} \leq \Pi_1 - \gamma_1 N_C, \tag{7}$$

$$\frac{dN_V}{dt} \leq \Pi_2 - (\gamma_2 + u_3)N_V. \tag{8}$$

Under the application of the Laplace transform, it simplifies to yield

$$sN_C(s) - N_{C_0} \leq \frac{\Pi_1}{s} - \gamma_1 N_C(s),$$

$$sN_V(s) - N_{V_0} \leq \frac{\Pi_2}{s} - (\gamma_2 + u_3)N_V(s),$$

which may be resolved for $N_C(s)$ and $N_V(s)$ to obtain

$$N_C(s) \leq \frac{\Pi_1}{s\gamma_1} - \frac{\Pi_1}{(s+\gamma_1)\gamma_1} + \frac{N_{C_0}}{(s+\gamma_1)},$$

$$N_V(s) \leq \frac{\Pi_2}{s(\gamma_2+u_3)} - \frac{\Pi_2}{(s+\gamma_2+u_3)(\gamma_2+u_3)} + \frac{N_{V_0}}{(s+\gamma_2+u_3)}.$$

The inverse Laplace transform is used to get the following solutions:

$$N_C(s) \leq \frac{\Pi_1}{\gamma_1}(1 - e^{-\gamma_1 t}) + N_C(0)e^{-\gamma_1 t},$$

and

$$N_V(s) \leq \frac{\Pi_2}{(\gamma_2+u_3)}\left(1 - e^{-(\gamma_2+u_3)t}\right) + N_V(0)e^{-(\gamma_2+u_3)t}.$$

It may be articulated that

$$\lim_{t\to\infty} N_C(s) \leq \frac{\Pi_1}{\gamma_1} \text{ and } \lim_{t\to\infty} N_V(s) \leq \frac{\Pi_2}{(\gamma_2+u_3)}.$$

Therefore, it can be asserted that solution $X(t)$ is bounded for any $t \geq 0$.

For the cattle model (1) to be useful in epidemiology, it is significant to show that the system's case variables are always non-negative when $t > 0$. The solution of the cattle model (1) with non-negative beginning conditions will stay positive at all times $t > 0$.

4. Stability analysis and equilibrium points

4.1 Disease-free equilibrium point (DFE)

A disease-free equilibrium is a state where a population is devoid of disease. In the lack of LSD, $I_C = R = I_V = 0$**.** Setting all derivatives of the LSD model (1) to zero and establishing $I_C = R = I_V = 0$, DFE is defined as

$$E_0 = \left(\frac{\Pi_1}{u_1+\gamma_1+\varepsilon}, \frac{(u_1+\varepsilon)\Pi_1}{\gamma_1(u_1+\gamma_1+\varepsilon)}, 0, 0, \frac{\Pi_2}{u_3+\gamma_2}, 0\right).$$

4.2 Computation of R_0

This part explains how R_0 for the LSD model (1) is calculated utilizing the methodology outlined in [33]. To do this, the subsequent matrices are derived.

Define $x_i = I_C, I_V$, a new infection matrix ($\mathcal{F}_i$):

$$\mathcal{F}_i = \begin{bmatrix} \frac{(1-u_2)\eta_1 S_C I_C}{N_C} + \frac{(1-u_3)\eta_2 S_C I_V}{N_C} \\ \frac{(1-u_3)\eta_3 S_V I_C}{N_C} \end{bmatrix},$$

where $N_C(t) = S_C(t) + V_C(t) + I_C(t) + R_C(t)$ and the transition matrix (V_i):

$$V_i = \begin{bmatrix} (\rho + \gamma_1 + \sigma + u_2) I_C \\ (\gamma_2 + u_3) I_V \end{bmatrix}.$$

The Jacobian of $\mathcal{F}_i$ and V_i

$$F = \frac{\partial \mathcal{F}_i(E_0)}{\partial x_i} = \begin{bmatrix} \frac{(1-u_2)\eta_1 S_C^*}{N_C} & \frac{(1-u_3)\,\eta_2\, S_C^*}{N_C} \\ \frac{(1-u_3)\,\eta_3\, S_V^*}{N_C} & 0 \end{bmatrix} \text{ and } V = \frac{\partial V_i(E_0)}{\partial x_i} = \begin{bmatrix} \rho + \gamma_1 + \sigma + u_2 & 0 \\ 0 & \gamma_2 + u_3 \end{bmatrix}.$$

The next-generation matrix is $K = FV^{-1}$,

$$K = \begin{bmatrix} \frac{(1-u_2)\eta_1 S_C^*}{(\rho + \gamma_1 + \sigma + u_2)} & \frac{(1-u_3)\eta_2 S_C^*}{(\gamma_2 + u_3)} \\ \frac{(1-u_3)\eta_3 S_V^*}{(\rho + \gamma_1 + \sigma + u_2)} & 0 \end{bmatrix},$$

where

$$S_C^* = \frac{\Pi_1}{u_1 + \gamma_1 + \varepsilon},\ S_V^* = \frac{\Pi_2}{u_3 + \gamma_2}.$$

Then, the reproduction number R_0 is given as

$$R_0 = \frac{1}{2}\frac{(1-u_2)\eta_1\gamma_1}{(\rho + \gamma_1 + \sigma + u_2)(u_1 + \gamma_1 + \varepsilon)}$$

$$+\sqrt{\left(\frac{(1-u_2)\eta_1\gamma_1}{2\,(\rho + \gamma_1 + \sigma + u_2)(u_1 + \gamma_1 + \varepsilon)}\right)^2 + \frac{(1-u_3)^2\,\eta_2\eta_3{\gamma_1}^2\Pi_2}{\Pi_1\,(u_3 + \gamma_2)^2(u_1 + \gamma_1 + \varepsilon)(\rho + \gamma_1 + \sigma + u_2)}},$$

$$R_0 = R_1 + R_2, \tag{9}$$

where

$$R_1 = \frac{(1-u_2)\eta_1\gamma_1}{2(\rho + \gamma_1 + \sigma + u_2)(u_1 + \gamma_1 + \varepsilon)},$$

$$R_2 = \sqrt{\left(\frac{(1-u_2)\,\eta_1\gamma_1}{2\,(\rho+\gamma_1+\sigma+u_2)(u_1+\gamma_1+\varepsilon)}\right)^2 + \frac{(1-u_3)^2\,\eta_2\eta_3{\gamma_1}^2\Pi_2}{\Pi_1\,(u_3+\gamma_2)^2(u_1+\gamma_1+\varepsilon)(\rho+\gamma_1+\sigma+u_2)}},$$

and

$$R_1^* = \frac{(1-u_2)\eta_1\gamma_1}{(\rho+\gamma_1+\sigma+u_2)(u_1+\gamma_1+\varepsilon)},$$

$$R_2^* = \frac{(1-u_3)^2\eta_2\eta_3{\gamma_1}^2\Pi_2}{\Pi_1(u_3+\gamma_2)^2(u_1+\gamma_1+\varepsilon)(\rho+\gamma_1+\sigma+u_2)}.$$

The formulas R_1^* and R_2^* are modified to derive the expression for R_0 in the subsequent analysis of model (1).

4.3 Local stability of disease-free equilibrium

Theorem 4. The DFE point E_0 of *LSD* model (1) is asymptotically stable under local conditions if $R_0^* < 1$ and unstable otherwise.

Proof. The Jacobian matrix of the *LSD* model (1) is computed at the disease-free equilibrium E_0

$J(E_0) =$

$$\begin{pmatrix} -u_1-\gamma_1-\epsilon & 0 & -\frac{(1-u_2)\gamma_1\eta_1}{u_1+\gamma_1+\epsilon} & \alpha & 0 & -\frac{(1-u_3)\gamma_1\eta_2}{u_1+\gamma_1+\epsilon} \\ u_1+\epsilon & -\gamma_1 & 0 & 0 & 0 & 0 \\ 0 & 0 & -u_2-\gamma_1-\left(\frac{(-1+u_2)\,\eta_1\gamma_1}{u_1+\gamma_1+\epsilon}\right)-\rho-\sigma & 0 & 0 & \frac{(1-u_3)\gamma_1\eta_2}{u_1+\gamma_1+\epsilon} \\ 0 & 0 & u_2+\rho & -\alpha-\gamma_1 & 0 & 0 \\ 0 & 0 & -\frac{S_V^*(1-u_3)\gamma_1\eta_3}{S_C^*\,(u_1+\gamma_1+\epsilon)} & 0 & -u_3-\gamma_2 & 0 \\ 0 & 0 & \frac{S_V^*(1-u_3)\gamma_1\eta_3}{S_C^*(u_1+\gamma_1+\epsilon)} & 0 & 0 & -u_3-\gamma_2 \end{pmatrix}.$$

The eigenvalues of the matrix $J(E_0)$ are calculated and yield

$$\lambda_1 = -\gamma_1,\ \lambda_2 = -u_3-\gamma_2, \lambda_3 = -u_1-\gamma_1-\epsilon\,, \lambda_4 = -\alpha-\gamma_1.$$

The other two roots can be derived from the quadratic characteristic equation provided by

$$\lambda^2 + \lambda a_1 + a_2 = 0, \tag{10}$$

where

$$a_1 = (u_3+\gamma_2) + (u_2+\gamma_1+\rho+\sigma)(1-R_1^*),$$

$$a_2 = (u_3+\gamma_2)(u_2+\gamma_1+\rho+\sigma)(1-R_0^*),$$

$$R_0^* = {R_0}^2 + 2R_1(1-R_0).$$

It is seen in the characteristic equation (10) that all related coefficients $a_i > 0$ for $i = 1{,}2$ if and only if $R_0^* < 1$. Using Routh–Hurwitz criteria [24,34], it is simple to demonstrate that from the Hurwitz matrix is $H_2 = \begin{pmatrix} a_1 & 1 \\ 0 & a_2 \end{pmatrix}$, and $|H_2| = a_1a_2 > 0$.

The model's disease-free equilibrium is asymptotically stable locally when $R_0^* < 1$, and unstable otherwise.

4.4 Endemic equilibrium point (EE)

The endemic equilibrium, represented by E^*, is the stable solution that arises from the sustained presence of disease within the community. The EE is denoted as $E^* = ({S_C}^*, V^*, {I_C}^*, {R_C}^*, {S_V}^*, {I_V}^*)$, when articulated about the forces of infection β_c^* and β_v^*, where

$$ {S_C}^* = \frac{\beta_3 \Pi_1}{\beta_1\beta_3 + (-\alpha + \beta_3)\beta_c + \beta_3\gamma_1}, $$

$$ V_c^* = \frac{\beta_1\beta_3\Pi_1}{(-\alpha + \beta_3)\beta_c\gamma_1 + \gamma_1(\beta_1\beta_3 + \beta_3\gamma_1)}, $$

$$ I_c^* = \frac{\beta_3\beta_c\Pi_1}{(-\alpha + \beta_3)\beta_c(\beta_2 + \gamma_1 + \sigma) + (\beta_1\beta_3 + \beta_3\gamma_1)(\beta_2 + \gamma_1 + \sigma)}, $$

$$ R_c^* = \frac{\beta_c\Pi_1}{\beta_1\beta_3 + (-\alpha + \beta_3)\beta_c + \beta_3\gamma_1}, $$

$$ S_V^* = \frac{\Pi_2}{\beta 4 + \beta v}, $$

$$ I_V^* = \frac{\beta_V\,\Pi_2}{\beta_4(\beta_4 + \beta_V)}, $$

where

$$ \beta_C = \frac{(1-u_2)\,\eta_1 I_c^*}{N_C} + \frac{(1-u_3)\eta_2 I_V^*}{N_C}, \qquad \beta_V = \frac{(1-u_3)\eta_3 I_c^*}{N_C}, $$

$$ \beta_1 = (\epsilon + u_1), \beta_2 = (\rho + u_2), \qquad \beta_3 = (\alpha + \gamma_1), \beta_4 = (\gamma_2 + u_3). $$

4.5 Asymptotic stability of the endemic equilibrium point

Theorem 5. The endemic equilibrium of the *LSD* model (1) is locally asymptotically stable if it satisfies the Routh–Hurwitz criteria and under the conditions of $\beta_C, \beta_V > 0$, and $\beta_3 > \alpha$.

Proof. The Jacobian matrix for the LSD system (1) at E^* is derived as follows:

$$ J(E^*) = \begin{pmatrix} -\beta_1 - \beta_C - \gamma_1 & 0 & 0 & \alpha & 0 & 0 \\ \beta_1 & -\gamma_1 & 0 & 0 & 0 & 0 \\ \beta_C & 0 & -\beta_2 - \gamma_1 - \sigma & 0 & 0 & 0 \\ 0 & 0 & \beta_2 + \gamma_1 + \sigma & -\beta_3 & 0 & 0 \\ 0 & 0 & 0 & 0 & -\beta_4 - \beta_V & 0 \\ 0 & 0 & 0 & 0 & \beta_V & -\beta_4 \end{pmatrix}. $$

The eigenvalues of the matrix $J(E^*)$ are calculated, and three of the eigenvalues are

$$ \lambda_1 = -\beta_4, \lambda_2 = -\beta_4 - \beta_V, \lambda_3 = -\gamma_1. $$

The characteristic equation for determining the remaining three eigenvalues is expressed as

$$\lambda^3 + \mathrm{b}_1\lambda^2 + \mathrm{b}_2\lambda + \mathrm{b}_3 = 0, \tag{11}$$

where

$$\mathrm{b}_1 = \beta_1 + \beta_2 + \beta_3 + \beta_C + 2\gamma_1 + \sigma,$$

$$\mathrm{b}_2 = (\beta_3+\gamma_1)\beta_C + 2\beta_3\gamma_1 + {\gamma_1}^2 + (\beta_3 + \beta_C + \gamma_1)(\beta_2 + \sigma) + \beta_1(\beta_2 + \beta_3 + \gamma_1 + \sigma),$$

$$\mathrm{b}_3 = \big((\beta_1 + \gamma_1)\beta_3 + (-\alpha + \beta_3)\,\beta_C\big)(\beta_2 + \gamma_1 + \sigma).$$

From the characteristic equation (11), the subsequent Hurwitz matrix is derived from the polynomial equation

$$H_3 = \begin{pmatrix} \mathrm{b}_1 & 1 & 0 \\ \mathrm{b}_3 & \mathrm{b}_2 & \mathrm{b}_1 \\ 0 & 0 & \mathrm{b}_3 \end{pmatrix},$$

where

$$\mathrm{b}_1 = \beta_1 + \beta_2 + \beta_3 + \beta_C + 2\gamma_1 + \sigma > 0,$$

$$\mathrm{b}_2 = (\beta_3+\gamma_1)\beta_C + 2\beta_3\gamma_1 + {\gamma_1}^2 + (\beta_3 + \beta_C + \gamma_1)(\beta_2 + \sigma) + \beta_1(\beta_2 + \beta_3 + \gamma_1 + \sigma) > 0,$$

$$\mathrm{b}_3 = \big((\beta_1 + \gamma_1)\beta_3 + (-\alpha + \beta_3)\beta_C\big)(\beta_2 + \gamma_1 + \sigma) > 0 \text{ if and only if } \beta_3 > \alpha.$$

Based on the criteria of Routh–Hurwitz, $|H_3| > 0$ if $b_1, b_2, b_3 > 0$ and $\mathrm{b}_1\mathrm{b}_2 > \mathrm{b}_3$.

Given that all parameters and variables are positive, the characteristic Eq (11) has negative real parts if the Routh-Hurwitz is satisfied, and the LSD model (1) at E^* is asymptotically stable.

5. Sensitivity analysis

Sensitivity analysis enables researchers to examine the sensitivity index of each of the R_0 parameters. It provides several significant conclusions, such as whether raising a particular value of the parameter will be raise the dependent variable's value, R_0, or cause it to fall to a particular value. Performing a comprehensive study is essential to developing the best disease control plans. This process makes it possible to pinpoint the precise R_0 characteristics that are most sensitive to it. A parameter can be claimed to be highly sensitive if its sensitivity index reading is high. The normalized sensitivity technique, which was established and implemented, is used in [31,35] to ascertain the sensitivity index of every parameter. Parameters with a high sensitivity index might be thought of as control variables that could aid in lowering the R_0 value so that the illness is no longer an epidemic. The next formula is used to calculate a parameter's sensitivity index:

$$\Upsilon_{\varpi}^{R_0} = \frac{\partial R_0}{\partial \varpi} \times \frac{\varpi}{R_0}, \tag{12}$$

where ϖ represents model parameters in which interest is taken.

This method is used to calculate the sensitivity measures for each parameter are calculated in R_0, and the results of this computation are represented graphically in Figure 2, where the ascending and descending bars indicate the direct and indirect relationships between the parameters and R_0, respectively.

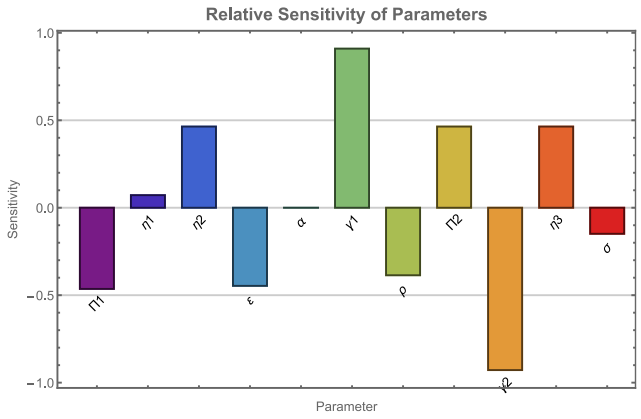

Figure 2. The sensitivity index for model parameters.

It is clear from Figure 2 that the parameters that have a positive sensitivity index such as γ_1, η_2, η_3, Π_2, and η_1 have a direct effect on the R_0, i.e., that an increase or decrease in the value of these parameters causes an increase or decrease in the value of R_0, which leads to the spread or reduction of the disease. In contrast, the parameters that have a negative sensitivity index, such as γ_2, Π_1, ε, ρ, and σ have an inverse effect on the increase or decrease in the value of the R_0. Since parameters η_1, η_2, and η_3 are related to the contact rate infected or susceptible cattle with the susceptible or infected vector, quarantining and treating infected cattle will limit virus transmission, and spraying the infected vector will also reduce the spread of the virus, which may be effective strategies to limit the spread of the disease. Moreover, the vaccination rate ε has a significant inverse effect on the R_0, which makes vaccination an effective strategy to reduce the spread of the disease. The behavior of R_0 with related parameters is presented in Figure 3.

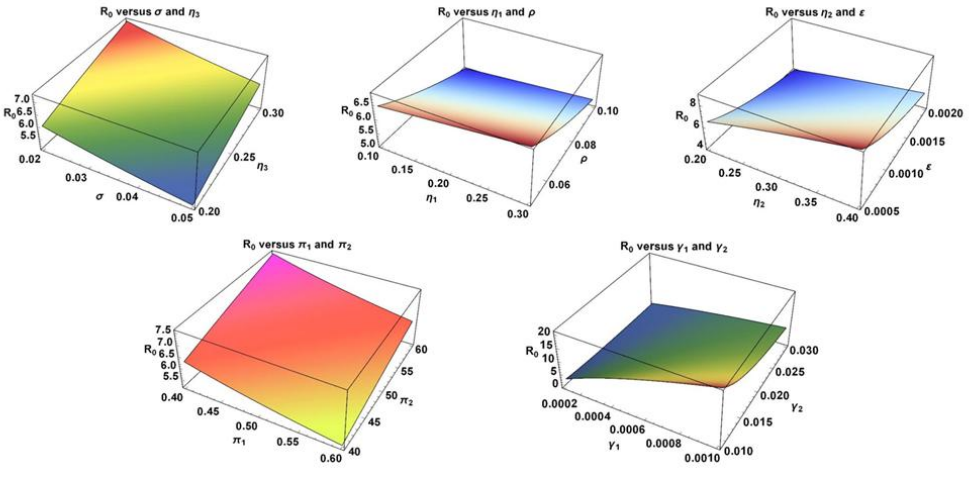

Figure 3. The relationship curves of R_0 against model parameters.

6. Optima control analysis

Determining a control law for a specified system that achieves a particular criterion is known as optimal control. A control variable and a function of state are both components of a control issue. A collection of differential equations outlining the control variables' paths that minimize the cost function is known as an optimal control. The control can be obtained using the Pontryagin's maximum principles (a necessary optimality condition) [36]. Thus, the optimal control theory is the most suitable mathematical theory for tackling issues involving deploying the best choice to accomplish a specific objective. Since this boundary-value problem results from taking the derivative of a Hamiltonian, it has a unique structure.

In this section, I formulate an optimal control issue that contains three control variables that are dependent on time, which are defined as vaccination control measures (u_1), treatment measures and quarantine of infected cattle (u_2), and pesticide spray measures for vectors (u_3) for controlling the transmission dynamics of LSD disease. To accomplish this, the objective function that incorporates both the controls and infected state variables is defined as follows:

$$\text{Minimize } J(u_1,u_2,u_3) = \int_0^T \left(A_1 I_C + A_2 I_V + \frac{1}{2}(B_1 u_1^2 + B_2 u_2^2 + B_3 u_3^2)\right) dt, \tag{13}$$

where the nonnegative constants A_1, A_2 and B_1, B_2, B_3 stand for the weights of the state variables and control measures, respectively. Moreover, the objective functional satisfies the following properties [37]:

(1) The control set and associated state variables are nonempty.

(2) The state variables and controls are nonnegative.

(3) The objective functional in the control pair satisfies the necessary convexity.

(4) The state system meets the Lipschitz property relating to the state variables, and the state solutions are bounded.

(5) The control set $\mho = \{u_1, u_2, u_3 : 0 \le u_1, u_2, u_3 \le 1,\ t \in [0,T]\}$ is compact.

To establish the requisite optimality criteria derived from Pontryagin's maximum principle, the Hamiltonian needs to be constructed (H) as the following form:

$$H = A_1 I_C + A_2 I_V + \frac{1}{2}(B_1 u_1^2 + B_2 u_2^2 + +B_3 u_3^2) + p_1\left(\Pi_1 - \frac{(1-u_2)\,\eta_1\, S_C\, I_C}{N_C} - \frac{(1-u_3)\,\eta_2\, S_C\, I_V}{N_C} - (\varepsilon + \gamma_1 + u_1)S_C\ + \alpha R_C\right) + p_2\left((\varepsilon + u_1)S_C\ - \gamma_1 V_C\right) + p_3\left(\frac{(1-u_2)\,\eta_1\, S_C\, I_C}{N_C} + \frac{(1-u_3)\,\eta_2\, S_C\, I_V}{N_C} - (\rho + \gamma_1 + \sigma + u_2)I_C\right) + p_4\left((\rho + u_2)I_C - (\alpha + \gamma_1)R_C\right) + p_5\left(\Pi_2 - \frac{(1-u_3)\,\eta_3\, S_V\, I_C}{N_C} - (\gamma_2 + u_3)S_V\right) + p_6\left(\frac{(1-u_3)\,\eta_3\, S_V\, I_C}{N_C} - (\gamma_2 + u_3)I_V\right), \tag{14}$$

where $p_k; k = 1,2,\ldots,6$ are adjoint variables. By deriving the Hamiltonian concerning the state variables and using the following relation:

$$\frac{dp_k}{dt} = -\frac{\partial H}{\partial \chi_k};\ k = 1,2,\ldots,6,$$

where $\chi_k = (S_C,\ V_C,\ I_C,\ R_C, S_V,\ I_V)$.

The following system of adjoint variables is derived:

$$\frac{dp_1}{dt} = \left(\frac{(1-u_2)\eta_1 I_C}{N_C} + \frac{(1-u_3)\eta_2 I_V}{N_C}\right)(p_1 - p_3) + (\epsilon + u_1)(p_1 - p_2) + \gamma_1 p_1,$$

$$\frac{dp_2}{dt} = \gamma_1 p_2,$$

$$\frac{dp_3}{dt} = -A_1 + \frac{(1-u_2)\eta_1 S_C}{N_C}(p_1 - p_3) + \frac{(1-u_3)\eta_3 S_V}{N_C}(p_5 - p_6) + (\rho + u_2)(p_3 - p_4) + (\sigma + \gamma_1)p_3,$$

$$\frac{dp_4}{dt} = \alpha(p_4 - p_1) + \gamma_1 p_4,$$

$$\frac{dp_5}{dt} = \frac{(1-u_3)\eta_3 I_C}{N_C}(p_5 - p_6) + (\gamma_2 + u_3)p_5,$$

$$\frac{dp_6}{dt} = -A_2 + \frac{(1-u_3)\,\eta_2\, S_C}{N_C}(p_1 - p_3) + (\gamma_2 + u_3)p_6, \tag{15}$$

subject to the terminal conditions $p_k(T) = 0; k = 1, 2, 3, 4, 5, 6$.

Further, the optimal controls under the max-min bounds are given by:

$$u_1^* = max\left\{0, min\left\{1, \frac{S_C(p_1 - p_2)}{B_1}\right\}\right\},$$

$$u_2^* = max\left\{0, min\left\{1, \frac{\eta_1 S_C I_C(p_3 - p_1) + I_C N_C(p_3 - p_4)}{B_2 N_C}\right\}\right\},$$

$$u_3^* = max\left\{0, min\left\{1, \frac{\eta_2 S_C I_V(p_3 - p_1) + \eta_3 S_V I_C(p_6 - p_5) + N_C S_V p_5 + I_V\, N_C\, p_6}{B_3 N_C}\right\}\right\}. \tag{16}$$

7. Numerical simulation

In this section, I verify the theoretical findings discussed above through a numerical simulation presented in a graphical representation. Moreover, the optimal solutions to the proposed optimal control problem is presented and analyzed to determine the most reasonable solution for addressing the proposed problem. For this purpose, the tabular data shown in Table 1 is used in addition to the following initial values for the variables of status $S_C(0) = 1000$, $V_C(0) = 20$, $I_C(0) = 50$, $R_C(0) = 0$, $S_V(0) = 2000$, and $I_V(0) = 50$. The weight values used in this simulation are $A_1 = 1$, $A_2 = 2$, $B_1 = 0.02$, $B_2 = 0.01$, and $B_3 = 0.2$.

The following four cases are considered using various control variable combinations.

Case 1: Combination of vaccination, treatment with the quarantine of infected cattle, and pesticide spray for vector control measures (all suggested control measures, i.e., $u_1 \neq 0, u_2 \neq 0, u_3 \neq 0$).

This case integrates all suggested control measures to reduce the transmission of LSD. The behavior of the model compartments with and without controls and the control function are presented in Figure 4. When vaccination procedures are applied, infected cattle are isolated with treatment, and the vector is sprayed; an increase in the vaccinated and recovered categories is observed, along with a noticeable decrease in infected cattle and the vector. Moreover, as it appears from the control profile, in the case of merging the proposed controls, the period of the controls being at their maximum potential is short before gradually decreasing. With the isolation of infected animals and their treatment, in addition to spraying the vectors, vaccination is needed only in the first days of the disease's spread. After that, it can be gradually reduced.

Case 2: Combination only between treatment with quarantine of infected cattle and pesticide spray for vector control measures (i.e., $u_1 = 0, u_2 \neq 0, u_3 \neq 0$).

In this case, procedures are applied to isolate and treat infected cattle and spray vectors without using procedures to vaccinate susceptible cattle. The behavior of the system variables and the priorities of the applied controls is depicted in Figure 5. A sharp decrease is noticed in the behavior of the curve of infected cattle and the vectors. Still, in the absence of vaccination procedures, the behavior of the curve of vaccinated cattle decreases, but not as it is in other cases. The control profile graph, shows that both applied controls should be implemented with maximum effort before gradually reducing vector spraying and isolation procedures at approximately 10 and 15 days from the control overlap period, respectively.

Case 3: Combination only between vaccination and pesticide spray for vector control measures (i.e., $u_1 \neq 0, u_2 = 0, u_3 \neq 0$).

In this case, vaccination of susceptible cattle and spraying vectors are used without considering the procedures for isolating and treating infected cattle. The simulation of this case is shown in Figure 6. The graphs show that the application of these controls has a noticeable effect in decreasing the incidence of infection cattle as well as vectors and increasing the number of vaccinated and recovered cattle. From the control profile, it appears that when combining these two controls, they should be used at maximum effort at the beginning of the overlap period and then gradually reduce the vaccination procedures at approximately 20 days while continuing to use vector spraying at maximum effort before gradually reducing it at approximately 25 days of the control period.

Case 4: Combination only between vaccination and treatment with quarantine of infected cattle control measures (i.e., $u_1 \neq 0, u_2 \neq 0, u_3 = 0$).

I focus on applying only vaccination and isolation of infected cattle and treatment without of measures of spraying vectors. The behavior of state variables in control and uncontrolled cases, in addition to the control profile, is presented in Figure 7. Applying these control measures results in a considerable decrease diseased cattle and vectors, and a major percentage of the herd recovers, as shown in Figure 7. Thus, this case is effective in reducing the LSD, according to the results, but vaccinating the susceptible cattle and isolation of infected cattle and treatment, particularly early in the epidemic, should be applied at maximum efforts almost until the end of the overlap period, as shown in the control profile graph.

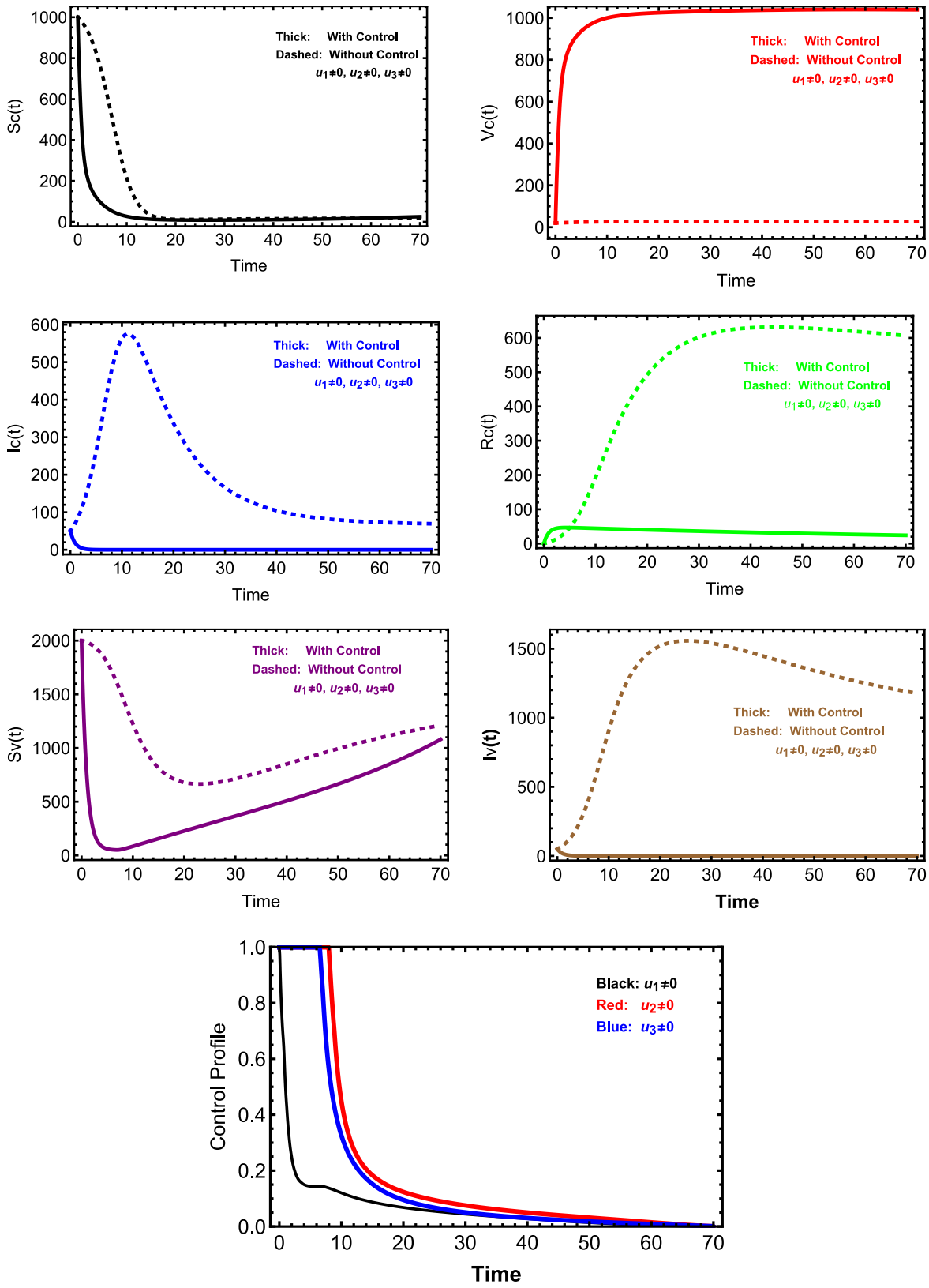

Figure 4. The influence of case 1 on state variables and the behavior of the control profile.

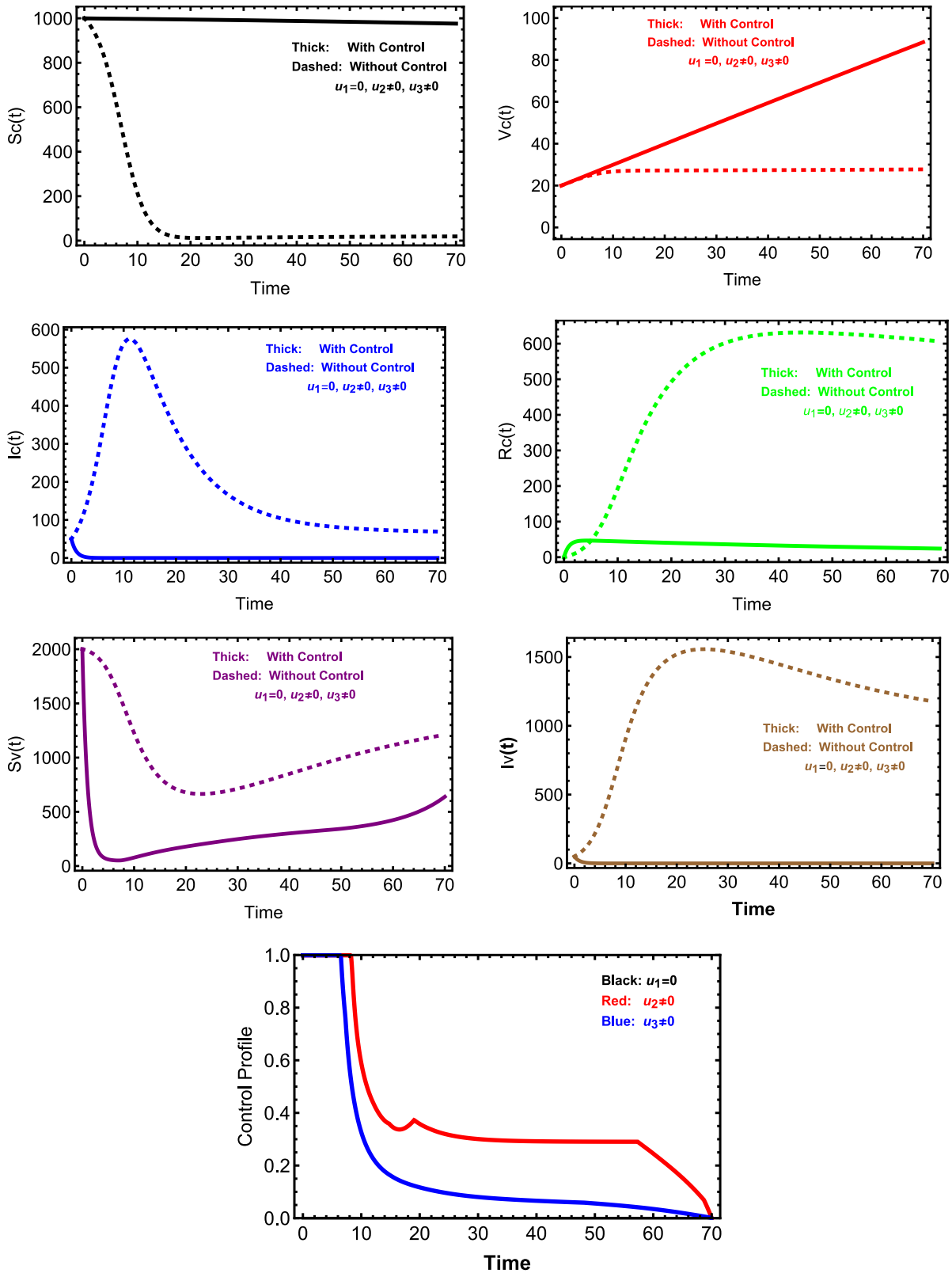

Figure 5. The influence of case 2 on state variables and the behavior of the control profile.

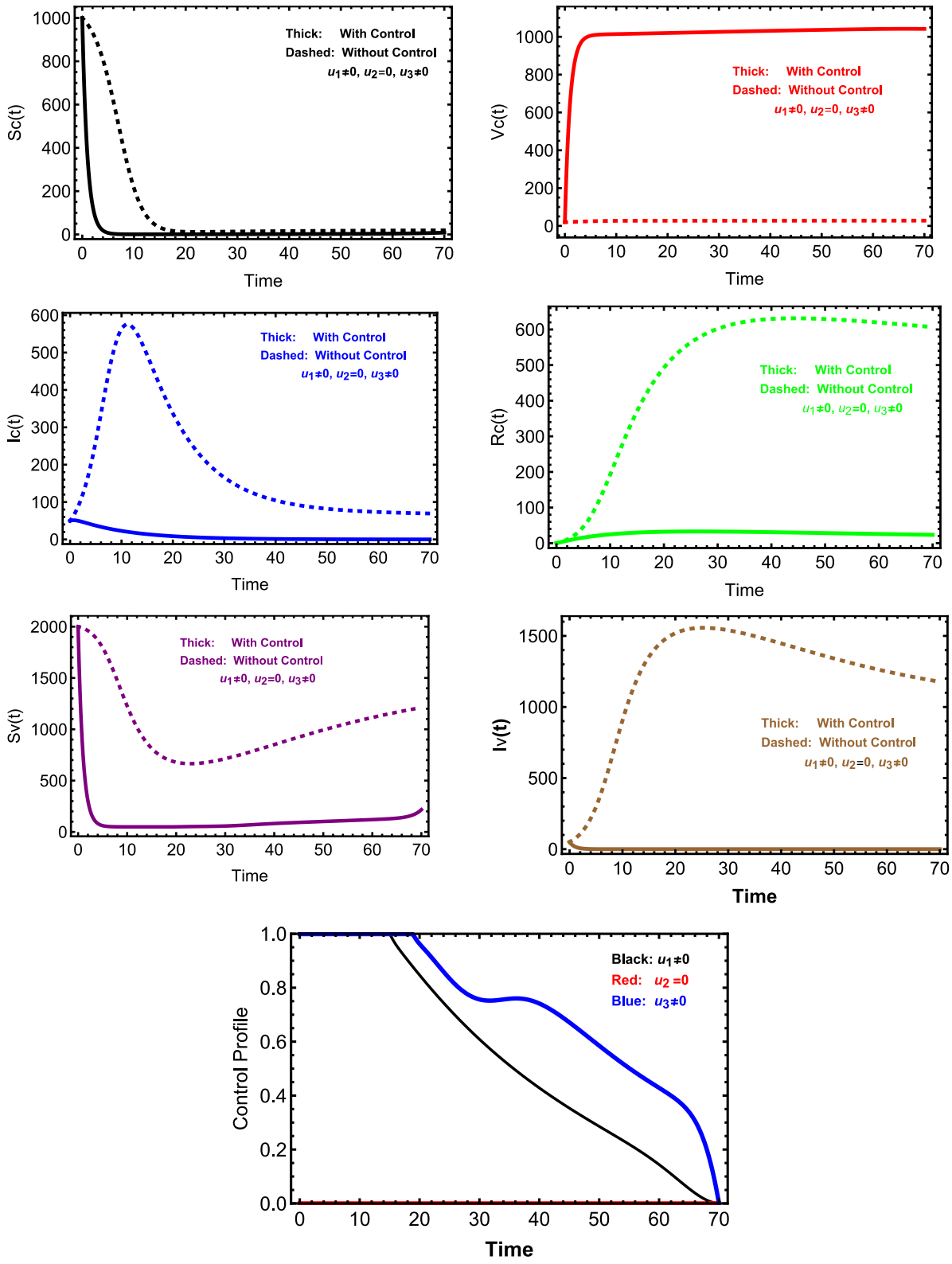

Figure 6. The effect of case 3 on the state variables and the behavior of the control profile.

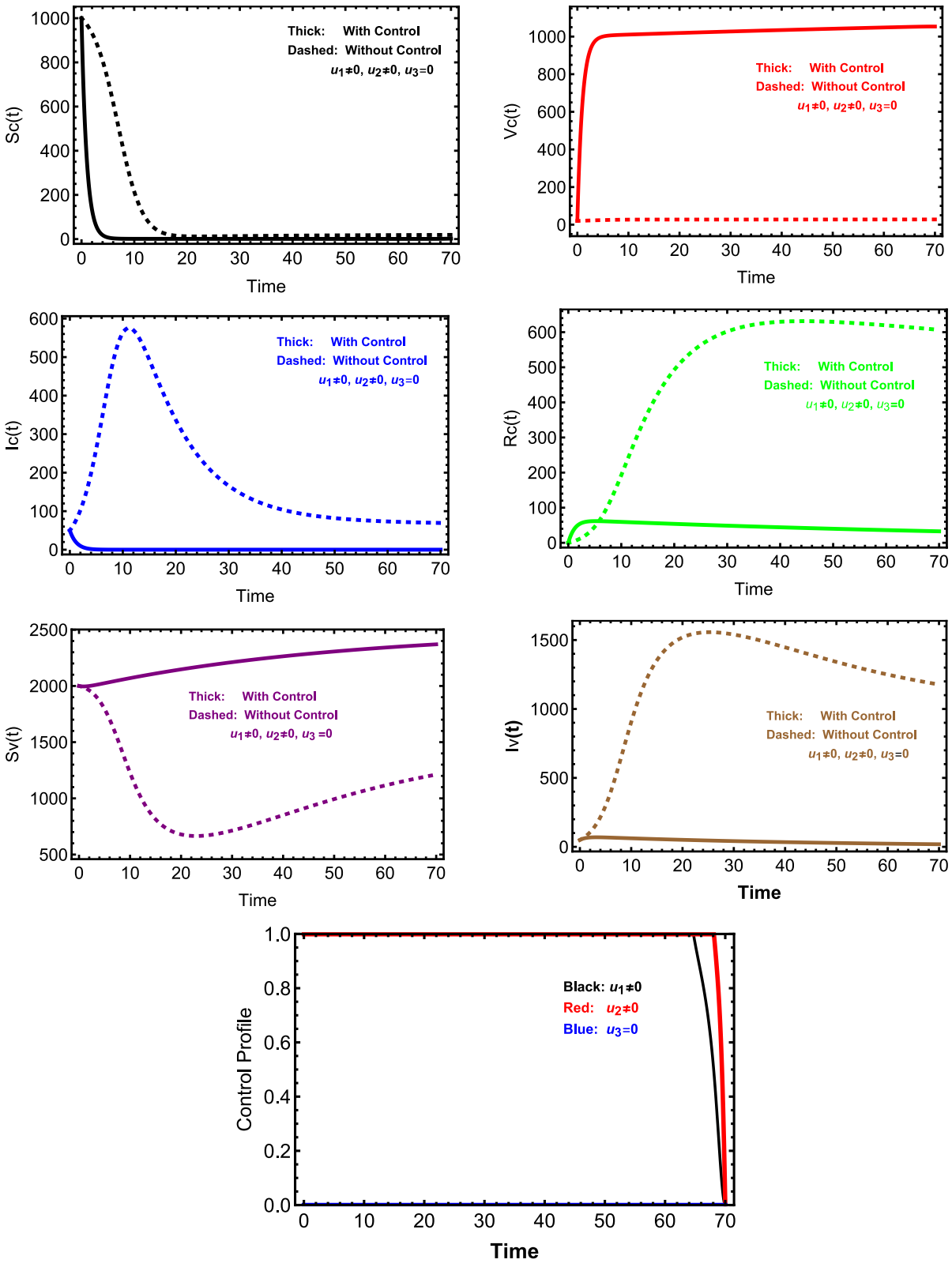

Figure 7. The influence of case 4 on state variables and the behavior of the control profile.

8. Conclusions

In this paper, I aim to develop a mathematical model that simulates the dynamics of disease transmission of LSD in cattle. The approach of the optimal control was used. The Runge-Kutta method from the fourth order was used to solve the numerical system. The stability of the mathematical model was analyzed. A sensitivity analysis was performed, and the results showed that the parameters exhibiting the highest sensitivity are the rate of natural death from vector insects and the vaccination rate. The optimal control theory was used to identify optimal strategies to reduce disease propagation. The following points represent the most important results of the research, which are as follows:

- The parameters with the highest sensitivity are the natural mortality rate of vector insects and the vaccination rate.
- Combining treatment, vaccination, and pesticide spraying contributes significantly reduces the rate of infected cases and increases the rate of recovered cases.
- Isolating infected animals and completing treatment reduces the spread of the disease among the sample.
- Covering the vector insects with pesticides significantly reduces disease transmission through vectors.

These outputs provide important indicators for those responsible for decision-making to control this disease and develop strategies to reduce the economic losses resulting from its spread.

The limitation of this study is that the proposed model is a classical ODE model, which does not account for memory effects that can be captured by fractional-order models. Additionally, empirical validation with real-world outbreak data was limited due to data unavailability. For future studies, researchers may address these aspects using advanced modeling frameworks.

Use of Generative-AI tools declaration

The author declares she has not used Artificial Intelligence (AI) tools in the creation of this article.

Acknowledgments

The author is thankful to the Deanship of Graduate Studies and Scientific Research at University of Bisha for supporting this work through the Fast-Track Research Support Program.

Conflict of interest

The author declares there is no conflict of interest.

References

1. A. Kononov, P. Prutnikov, I. Shumilova, S. Kononova, A. Nesterov, O. Byadovskaya, et al., Determination of lumpy skin disease virus in bovine meat and offal products following experimental infection, *Transbound. Emerg. Dis.*, **66** (2019), 1332–1340. https://doi.org/10.1111/tbed.13158

2. X. Roche, A. Rozstalnyy, D. TagoPacheco, C. Pittiglio, A. Kamata, D. Beltran Alcrudo, et al., *Introduction and spread of lumpy skin disease in South, East and Southeast Asia: Qualitative risk assessment and management*, Rome: Food and Agriculture Organization of the United Nations, 2021.
3. Y. Narwal, S. Rathee, Fractional order mathematical modeling of lumpy skin disease, *Commun. Faculty Sci. Uni. Ankara Ser. A1 Math. Stat.*, **73** (2024), 192–210. https://doi.org/10.31801/cfsuasmas.1207144
4. N. Ntombela, M. Matsiela, S. Zuma, S. Hiralal, L. Naicker, N. Mokoena, et al., Production of recombinant lumpy skin disease virus A27L and L1R proteins for application in diagnostics and vaccine development, *Vaccine X*, **15** (2023), 100384. https://doi.org/10.1016/j.jvacx.2023.100384
5. A. Mazloum, A. Van Schalkwyk, S. Babiuk, E. Venter, D. B. Wallace, A. Sprygin, Lumpy skin disease: history, current understanding and research gaps in the context of recent geographic expansion, *Front. Microbiol.*, **14** (2023), 1266759. https://doi.org/10.3389/fmicb.2023.1266759
6. L. Khan, I. A. Khan, M. Gul, M. B. Riaz, A. Khan, M. Saleem, et al., A comprehensive review on lumpy skin disease, *Pure Appl. Biol.*, **13** (2024), 341–350. https://doi.org/10.19045/bspab.2024.130031
7. E. Renald, J. Buza, J. M. Tchuenche, V. G. Masanja, The role of modeling in the epidemiology and control of lumpy skin disease: a systematic review, *Bull. Natl. Res. Centre*, **47** (2023), 141. https://doi.org/10.1186/s42269-023-01111-z
8. W. Ahmad, M. Abbas, Effect of quarantine on transmission dynamics of Ebola virus epidemic: a mathematical analysis, *Eur. Phys. J. Plus*, **136** (2021), 355. https://doi.org/10.1140/epjp/s13360-021-01360-9
9. D. Baleanu, F. A. Ghassabzade, J. J. Nieto, A. Jajarmi, On a new and generalized fractional model for a real cholera outbreak, *Alex. Eng. J.*, **61** (2022), 9175–9186. https://doi.org/10.1016/j.aej.2022.02.054
10. M. D. Ahmad, M. Usman, A. Khan, M. Imran, Optimal control analysis of Ebola disease with control strategies of quarantine and vaccination, *Infect. Dis. Poverty*, **5** (2016), 72. https://doi.org/10.1186/s40249-016-0161-6
11. F. Agusto, Optimal chemoprophylaxis and treatment control strategies of a tuberculosis transmission model, *World J. Model. Simul.*, **5** (2009), 163–173.
12. A. I. K. Butt, M. Imran, S. Batool, M. A. Nuwairan, Theoretical analysis of a COVID-19 CF-fractional model to optimally control the spread of pandemic, *Symmetry*, **15** (2023), 380. https://doi.org/10.3390/sym15020380
13. A. Butt, W. Ahmad, M. Rafiq, D. Baleanu, Numerical analysis of Atangana-Baleanu fractional model to understand the propagation of a novel corona virus pandemic, *Alex. Eng. J.*, **61** (2022), 7007–7027. https://doi.org/10.1016/j.aej.2021.12.042
14. A. I. K. Butt, H. Aftab, M. Imran, T. Ismaeel, Mathematical study of lumpy skin disease with optimal control analysis through vaccination, *Alex. Eng. J.*, **72** (2023), 247–259. https://doi.org/10.1016/j.aej.2023.03.073
15. W. Molla, K. Frankena, M. De Jong, Transmission dynamics of lumpy skin disease in Ethiopia, *Epidemiol. Infect.*, **145** (2017), 2856–2863. https://doi.org/10.1017/S0950268817001637
16. R. Magori-Cohen, Y. Louzoun, Y. Herziger, E. Oron, A. Arazi, E. Tuppurainen, et al., Mathematical modelling and evaluation of the different routes of transmission of lumpy skin disease virus, *Vet. Res.*, **43** (2012), 1. https://doi.org/10.1186/1297-9716-43-1

17. S. Gubbins, A. Stegeman, E. Klement, L. Pite, A. Broglia, J. C. Abrahantes, Inferences about the transmission of lumpy skin disease virus between herds from outbreaks in Albania in 2016, *Prev. Vet. Med.*, **181** (2020), 104602. https://doi.org/10.1016/j.prevetmed.2018.12.008
18. Z. Stojmanovski, Space-time permutation model applied to the past outbreak data of lumpy skin disease in the Balkan Peninsula from August 2015 to July 2017, *Vet. Glasnik*, **72** (2018), 44–55. https://doi.org/10.2298/VETGL171027003S
19. B. Mat, M. S. Arikan, A. C. Akin, M. B. Çevrimli, H. Yonar, M. A. Tekindal, Determination of production losses related to lumpy skin disease among cattle in Turkey and analysis using SEIR epidemic model, *BMC Vet. Res.*, **17** (2021), 300. https://doi.org/10.1186/s12917-021-02983-x
20. V. Punyapornwithaya, O. Arjkumpa, N. Buamithup, N. Kuatako, K. Klaharn, C. Sansamur, et al., Forecasting of daily new lumpy skin disease cases in Thailand at different stages of the epidemic using fuzzy logic time series, NNAR, and ARIMA methods, *Prev. Vet. Med.*, **217** (2023), 105964. https://doi.org/10.1016/j.prevetmed.2023.105964
21. S. Moonchai, A. Himakalasa, T. Rojsiraphisal, O. Arjkumpa, P. Panyasomboonying, N. Kuatako, et al., Modelling epidemic growth models for lumpy skin disease cases in Thailand using nationwide outbreak data, 2021–2022, *Infect. Dis. Model.*, **8** (2023), 282–293. https://doi.org/10.1016/j.idm.2023.02.004
22. A. Elsonbaty, M. Alharbi, A. El-Mesady, W. Adel, Dynamical analysis of a novel discrete fractional lumpy skin disease model, *PDE Appl. Math.*, **9** (2024), 100604. https://doi.org/10.1016/j.padiff.2023.100604
23. W. F. Alfwzan, M. H. DarAssi, F. Allehiany, M. A. Khan, M. Y. Alshahrani, E. M. Tag-eldin, A novel mathematical study to understand the Lumpy skin disease (LSD) using modified parameterized approach, *Results Phys.*, **51** (2023), 106626. https://doi.org/10.1016/j.rinp.2023.106626
24. E. Renald, V. G. Masanja, J. M. Tchuenche, J. Buza, A deterministic mathematical model with non-linear least squares method for investigating the transmission dynamics of lumpy skin disease, *Healthcare Analyt.*, **5** (2024), 100343. https://doi.org/10.1016/j.health.2024.100343
25. H. Alrabaiah, M. A. Safi, M. H. DarAssi, B. Al-Hdaibat, S. Ullah, M. A. Khan, et al., Optimal control analysis of hepatitis B virus with treatment and vaccination, *Results Phys.*, **19** (2020), 103599. https://doi.org/10.1016/j.rinp.2020.103599
26. S. Ullah, M. A. Khan, Modeling the impact of non-pharmaceutical interventions on the dynamics of novel coronavirus with optimal control analysis with a case study, *Chaos Solitons Fract.*, **139** (2020), 110075. https://doi.org/10.1016/j.chaos.2020.110075
27. M. S. Abdo, K. Shah, H. A. Wahash, S. K. Panchal, On a comprehensive model of the novel coronavirus (COVID-19) under Mittag-Leffler derivative, *Chaos Solitons Fract.*, **135** (2020), 109867. https://doi.org/10.1016/j.chaos.2020.109867
28. A. Alderremy, J. Gómez-Aguilar, S. Aly, K. M. Saad, A fuzzy fractional model of coronavirus (COVID-19) and its study with Legendre spectral method, *Results Phys.*, **21** (2021), 103773. https://doi.org/10.1016/j.rinp.2020.103773
29. M. A. Khan, S. A. A. Shah, S. Ullah, K. O. Okosun, M. Farooq, Optimal control analysis of the effect of treatment, isolation and vaccination on hepatitis B virus, *J. Biol. Syst.*, **28** (2020), 351–376. https://doi.org/10.1142/S0218339020400057

30. A. I. K. Butt, Dynamical modeling of Lumpy skin disease using Atangana-Baleanu derivative and optimal control analysis, *Model. Earth Syst. Environ.*, **11** (2025), 27. https://doi.org/10.1007/s40808-024-02239-1
31. O. Falowo, J. Owolabi, O. Oludoun, R. Akingbade, Mathematical modelling of lumpy skin disease in dairy cow, *IOP Conf. Ser.: Earth Environ. Sci.*, **1219** (2023), 012007.
32. Lumpy Skin Disease Virus, Octavoscene, 2022. Available from: https://www.octavoscene.co.za/3497-2/.
33. K. Dietz, The estimation of the basic reproduction number for infectious diseases, *Stat. Meth. Med. Res.*, **2** (1993), 23–41. https://doi.org/10.1177/096228029300200103
34. M. Khan, K. Ali, E. Bonyah, K. Okosun, S. Islam, A. Khan, Mathematical modeling and stability analysis of Pine Wilt Disease with optimal control, *Sci. Rep.*, **7** (2017), 3115. https://doi.org/10.1038/s41598-017-03179-w
35. N. Chitnis, J. M. Hyman, J. M. Cushing, Determining important parameters in the spread of malaria through the sensitivity analysis of a mathematical model, *Bull. Math. Biol.*, **70** (2008), 1272–1296. https://doi.org/10.1007/s11538-008-9299-0
36. L.S. Pontryagin, *Mathematical theory of optimal processes*, London: Routledge, 2018.
37. H. M. Ali, I. G. Ameen, Save the pine forests of wilt disease using a fractional optimal control strategy, *Chaos Solitons Fract.*, **132** (2020), 109554. https://doi.org/10.1016/j.chaos.2019.109554

AIMS Press

© 2025 the Author(s), licensee AIMS Press. This is an open access article distributed under the terms of the Creative Commons Attribution License (http://creativecommons.org/licenses/by/4.0)